

MRI manifestations of persistent microvascular obstruction and acute left ventricular remodeling in an experimental reperfused myocardial infarction

Yuesong Yang¹, John J. Graham², Kim Connelly², Warren D. Foltz³, Alexander J. Dick⁴, Graham A. Wright^{1,5}

¹Imaging Research and Schulich Heart Program, Sunnybrook Health Sciences Centre, University of Toronto, Canada; ²Division of Cardiology, St. Michael's Hospital, University of Toronto, Canada; ³Radiation Medicine Program, Princess Margaret Hospital, University of Toronto, Canada; ⁴Division of Cardiology, Ottawa Heart Institute, Canada; ⁵Department of Medical Biophysics, University of Toronto, Canada

ABSTRACT

Purpose: To investigate varied manifestations of persistent microvascular obstruction (PMO) and acute left ventricular (LV) remodeling in an experimental reperfused myocardial infarction (MI) using MRI.

Methods: In eleven Yorkshire pigs an acute MI was produced through a 90-minute balloon occlusion of the middle left anterior descending coronary artery, followed by reperfusion. All animals underwent MRI examinations on a 1.5T system including a SSFP functional study, first pass myocardial perfusion (FPMP), T1 preparation Look-Locker and delayed contrast-enhanced MRI (DE-MRI). Imaging was performed immediately post-intervention (day 0) and at days 7-9. In four animals a repeat MRI examination was performed at day 2 as well. Upon study completion, animals underwent histological analysis including infarct assessment with triphenyltetrazolium chloride (TTC).

Results: Following reperfusion, Thrombolysis In Myocardial Infarction (TIMI) Flow grade 3 was achieved in all animals, demonstrated by repeat angiography following balloon deflation (day 0). Various MR appearances of PMO were noticed including predominance in the subendocardial region, a central core within the infarcted tissue and also multiple separate clusters. In ten of eleven animals PMO was demonstrated as a persistent hypo-enhanced area in FPMP and DE-MRI, and identified as bright regions in later T1 difference images. In one animal PMO was identified only at day 2. At day 7-9 PMO could be identified on early DE-MRI at 5-15 minutes post Gd injection but not on late DE-MRI and T1 difference images after 45-60 minutes post-contrast. A larger volume of PMO and MI at day 2 was noted in comparison to data from day 0 but the difference was not statistically significant. An increased end-diastolic LV volume (EDV) without changes in end-systolic LV volume (ESV) and LV mass at end-diastolic phase (LVM) was observed at day 7-9 in comparison to data from day 0. There was good correlation between the relative extent of persistent MO in the infarcted myocardium (% MO/MI) and EDV at day 7-9 ($r=0.83$, $n=10$, $P=0.003$). MI was confirmed in all animals by TTC staining and/or histology.

Conclusion: A variable MR appearance of persistent microvascular obstruction is observed during a short time course MRI study of reperfused acute MI. Acute negative LV remodeling was closely related to the relative extent of persistent microvascular obstruction within the infarct myocardium.

KEY WORDS

Microvascular obstruction; left ventricular remodeling; contrast-enhanced MRI; T1 difference image

Quant Imaging Med Surg 2012;2:12-20. DOI: 10.3978/j.issn.2223-4292.2011.12.02

No potential conflict of interest.

Corresponding to: Yuesong Yang, MD, PhD. Imaging Research, Sunnybrook Health Sciences Centre, S-605, 2075 Bayview Avenue, Toronto, Ontario, M4N 3M5, Canada. Tel: 1-416-480-6100 ext.89916; Fax: 1-416-480-5714. Email: ysyang@sri.utoronto.ca.

Submitted Dec 19, 2011. Accepted for publication Dec 26, 2011.

Available at <http://www.amepc.org/qims>

ISSN: 2223-4292 © AME Publishing Company. All rights reserved.



Introduction

Rapid restoration of coronary artery patency and blood flow to the jeopardized infarct myocardium through mechanical and/or pharmacological interventions is an essential therapeutic strategy in the clinical management of patients with acute myocardial infarction (AMI). However, at a tissue level, perfusion to the injured myocardium may be sub-optimal due to microvascular obstruction or no-reflow phenomenon despite patency in the infarct-related epicardial artery following percutaneous transluminal angioplasty and successful stent placement (1,2). Two primary mechanisms have been proposed as the causes of microvascular obstruction: one occurring at the capillary level characterized by myocardial necrosis and reperfusion damage, and the other occurring during the percutaneous coronary interventions due to distal embolization of plaque or thrombus (3,4). The histological findings from microvascular obstruction zones usually include endothelial cell damage plus intraluminal blockage by activated neutrophils, stagnation of red blood cells, and/or microthrombi with myocardial cell swelling (5-7). Early formation of microvascular obstruction has proven to be a strong predictor of worsening LV dysfunction or congestive heart failure, and adverse outcomes (8-11). Long-term persistence of microvascular obstruction is a predictor of increased scar thinning and infarct expansion resulting in negative remodeling (12).

With a growing body of evidence validating the significance of microvascular obstruction and the development of treatment strategies aimed at attenuating it (13), accurate detection of microvascular obstruction becomes an essential facet of clinical management (13,14). Magnetic resonance imaging (MRI) has become an important tool for the accurate diagnosis of microvascular obstruction and for following its evolution in experimental and clinical studies, largely because of its high contrast-noise ratio, reduced operator dependence and lack of ionizing radiation. First pass myocardial perfusion (FPMP) is the primary MRI method used to identify the presence of microvascular obstruction (9,10,15); and is often combined with delayed contrast-enhanced MRI (DE-MRI) to allow its quantification (8,16,17). In both FPMP and DE-MRI, microvascular obstruction appears as a negative contrast, or hypo-enhancement (15-17). Notably a modified T1 preparation MRI technique using Gd-DTPA has been proposed for the detection and characterization of microvascular obstruction with positive contrast in an animal model of experimental reperfused AMI (18).

As microvascular obstruction is a dynamic pathophysiological phenomenon, its appearance may be time-sensitive due to its

nature of progressive evolution in reperfused AMI. In this study we investigate various manifestations of persistent microvascular obstruction (PMO) and LV remodeling in experimental reperfused AMI using MRI over a short time course.

Materials and Methods

Animal preparation and procedures

Our Institutional Animal Care and Use Committee has reviewed and approved this study. All eleven Yorkshire pigs (22-30 kg) were on oral Metoprolol at a dose of 50 mg/day for 5 days ahead of the catheterization procedures. During catheterization and MRI studies all animals were anesthetized with an intravenous injection of a ketamine/atropine cocktail (35 mg/kg ketamine hydrochloride and 0.05 mg/kg atropine), intubated, ventilated with a volume respirator, masked at 5% halothane in oxygen, and maintained using 2% isoflurane. An infusion cocktail of amiodarone (150 mg) and lidocaine (2 mg/min) was used to reduce the risk of malignant tachyarrhythmias throughout the experiments.

All the interventions and scans were performed with the animals oriented supine in a radiolucent Plexiglas case. In each animal, via percutaneous trans-femoral access and under the guidance of x-ray fluoroscopy (OEC 9800; GE Healthcare), standard catheters were advanced to the left main coronary artery and baseline angiography performed. An angioplasty balloon (Maverick™, Boston Scientific, Natick, MA) was then placed into the left anterior descending coronary artery (LAD) distal to the second diagonal branch. Myocardial infarction was produced with a 90-minute occlusion by inflation of the angioplasty balloon at 4-6 atm to allow total occlusion of the middle LAD, with verification by angiography. After 90 minutes, the balloon was deflated and the LAD was reperfused for 120 to 150 minutes prior to MRI studies, and the patency of middle LAD was verified by repeat angiography.

MRI examinations

All MRI studies were performed on a GE 1.5T system (GE Healthcare, Milwaukee) post-intervention (day 0, n=11), at 48 hours (day 2, n=4), and on day 7-9 (n=11). A 5-inch surface or GP flex coil was used. Peripheral or ECG gating was realized using an *In vivo* Magnitude™ physiological monitor (*In Vivo* Corporation, Orlando, FL) through a plethysmography trace placed on the pig's tail or through electrodes placed on the anterior chest wall of the animal. The MRI study included a steady-state free precession (SSFP) functional study pre-contrast



and FPMP, DE-MRI, and T1 preparation post-contrast. For SSFP, 12-16 slices covering the whole left ventricle from the mitral valve to the apex were acquired with 5 mm slice thickness without gaps. Typical MR imaging parameters were as follows: TR=3.6-4.6 ms, TE=1.2-1.8 ms, flip angle=60°, field of view=23 cm, matrix=256×192, number of averages=6, cardiac phases per slice=20.

FPMP was performed immediately after a bolus injection of gadopentetate dimeglumine (Magnevist, Berlex Canada) at a dose of 0.2 mmol/kg using a power injector (Spectris; Medrad) at a rate of 4 ml/sec or by hand, then flushed with saline; the sequence was repeated for up to 4 minutes. A constant intravenous infusion of gadopentetate dimeglumine at a rate of 0.004 mmol/kg/min followed (19). Then DE-MRI (IR-prepared FGRE) was performed at two time points: early (5-15 minutes); and late (approximately 45 minutes) after gadopentetate dimeglumine infusion. Finally, a T1 preparation pulse sequence was applied around 60 minutes post-contrast at steady state. FPMP scans consisted of 3-6 short-axis oblique slices with 5 mm slice thickness with 0-2 mm gaps. The typical FPMP parameters were as follows: TR/TE=8.2/2.1 ms, flip angle=25°, TI approximately 210 ms, echo train length=4, matrix=128×128, field of view 23 cm, and number of averages=1. The DE-MRI studies spanned the whole left ventricle. The typical parameters for DE-MRI were as follows: TI varied from 200 to 300 ms dependent on the myocardium nulling, TR/TE=7.1/3.4 ms, flip angle=30°, slice thickness=5 mm without gaps, matrix=256×192-256, field of view=23×18 cm, and number of averages=6.

The T1 preparation technique is a modified Look-Locker pulse sequence that samples the approach to steady state with and without a preceding inversion at the same cardiac phase, producing 8 difference images from a set of spiral acquisitions in a train of 15-deg excitations at intervals of 120 ms (20,21). In these difference images, longer T1 values yield bright signal at later points (effectively longer TI). Typical MR parameters were as follows: twelve 3072-point spiral interleaves providing 1.07 mm in-plane resolution, cardiac gating across 3 or 4 RR intervals, number of averages=10, field of view=23 cm, and a single slice of 5 mm thickness. The chosen slice was selected from the short axis SSFP images based on the presence of appropriate wall motion abnormality.

SSFP, FPMP and DE-MRI analyses were conducted using Mass Plus software (MEDIS, Netherlands). T1 mapping was conducted using Xcinema (Stanford University) or Functool 2 (GE Healthcare). LV volumes at end-diastolic (EDV) and end-systolic phases (ESV) were calculated from the endocardial contours planimetered on short-axis oblique SSFP images by

use of a modified Simpson's rule through commercially available Mass plus software installed in the workstation (22). The epicardial contours of the left ventricle at the end-diastolic phase were manually segmented for LV mass calculation. Papillary muscles were included for the computation of left ventricular mass. A specific gravity of 1.05 was assumed for ventricular muscle.

Microvascular obstruction was defined as the persistent hypo-enhanced regions observed on FPMP and DE-MRI images and as persistent positive enhancement on subsequent T1 difference images. As the manifestation of microvascular obstruction may be time-sensitive (i.e. diminished area due to diffusion of gadolinium chelates from neighboring myocardium, or increased area due to progression of microvascular injury during early reperfusion (23)), the volume of microvascular obstruction was measured from sequential DE-MRI image sets as the sum of all of the hypo-enhanced areas at approximately 45 minutes post-contrast. DE-MRI images were selected as image sets for the measurement of microvascular obstruction because DE-MRI provided a better spatial resolution (1 mm² in-plane) than that of FPMP (3.2 mm² in-plane). To allow better comparison, myocardial infarction volume was measured from the same DE-MRI image sets as the sum of the areas of hypo- and hyper-enhancement.

All data are expressed as the mean value ± SD. Statistical significance in parameter changes was evaluated using the Student's paired t-test and P<0.05 was considered statistically significant.

Pathology

At the completion of MRI protocols, all animals were sacrificed and the heart excised. Each heart was filled with an inert polymer (Histomer, Histotech) and sliced manually into ~10 mm thick sections in short-axis oblique orientation starting from the apex. These sections were placed into a triphenyltetrazolium chloride (TTC) bath (2% TTC in saline at 37°C) for 15-20 minutes and photographed once the infarction was visible. Selected samples from infarcted and non-infarcted tissues were fixed in 10% neutral buffered formalin and processed for light microscopy histological analysis (hematoxylin and eosin staining).

Results

Manifestations of microvascular obstruction

Thrombolysis in Myocardial Infarction (TIMI) Flow grade 3 was achieved in all animals, as demonstrated through repeated



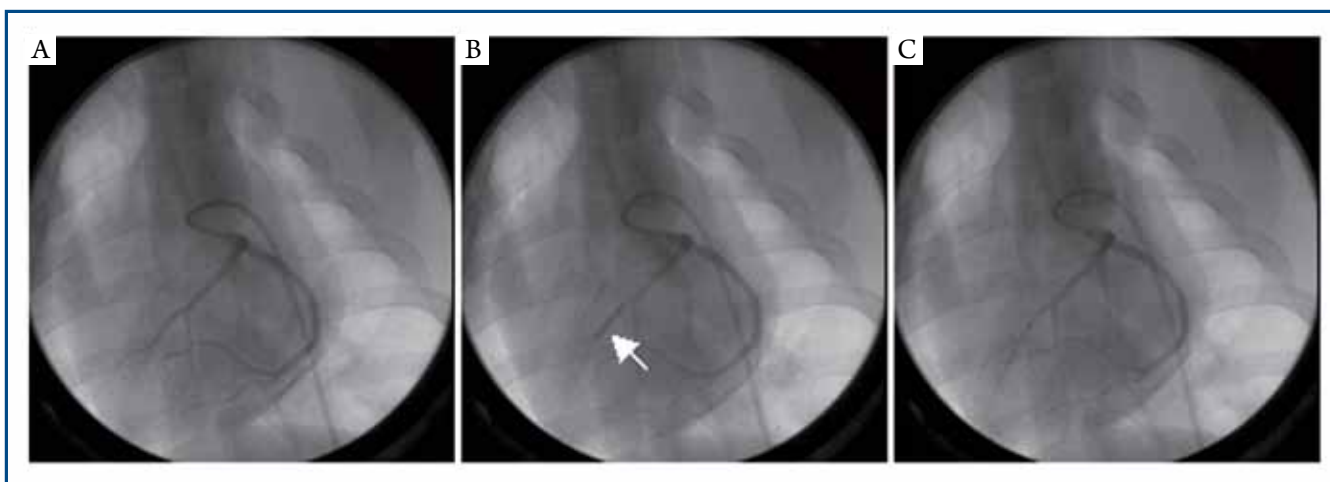


Figure 1. Angiography and TIMI Flow Grade. A: Pre-occlusion angiogram of middle LAD showing the patency of epicardial coronary artery; B: Balloon occlusion of middle LAD (arrow); C: Post-balloon release showing re-establishment of TIMI flow grade 3 (i.e. complete patency of epicardial coronary artery).

angiography on day 0 immediately following balloon deflation (Figure 1). Although TIMI flow grade 3 was present in all animals (implying microvascular integrity), in ten of eleven animals PMO was confirmed as a persistent hypo-enhanced area in FPMP and DE-MRI, and identified as bright regions in later T1 difference images. In one of these ten animals, PMO was identified only at day 2. The other nine animals showed PMO on day 0, which persisted at day 2 in the subset studied at that time point.

Various MR appearances of PMO were noticed on DE-MRI and T1 difference images including subendocardial distribution, central cores within the infarct tissue, and multiple separate foci (Figure 2). Using DE-MRI, PMO at day 0 was demonstrated in the majority of animals (9/10), as a hypo-enhanced core with a surrounding rim of high signal intensity infarct tissue. In contrast, on T1 difference images, PMO appeared as a positive enhancement core with a surrounding dark rim of infarcted myocardium. In one animal, at day 0, the PMO was first limited to the subendocardial region and at day 2 it evolved into the “core” pattern as mentioned above. In another animal, PMO appeared as multiple foci within the infarct tissue at day 0, with negative contrast on DE-MRI and positive contrast on T1 difference images. At day 7-9 PMO could be identified on early DE-MRI at 5-15 minutes post Gd injection but not on late DE-MRI and T1 difference images after 45-60 minutes post-contrast. All regions of myocardial infarction were demonstrated as transmural hyper-enhancement.

All animals had myocardial infarction confirmed by TTC staining and/or histological analysis.

Percent of PMO/MI and LV volumes

There was a trend toward increased volume of PMO and myocardial infarction at day 2 in comparison to day 0 (PMO volume at day 2 *vs.* day 0: 2.5 ± 1.9 *vs.* 1.9 ± 1.8 ml, $P=0.053$; MI volume at day 2 *vs.* day 0: 10.5 ± 3.3 *vs.* 9.9 ± 3.5 ml, $P=0.062$; $n=4$). At day 7-9 an increased end-diastolic LV volume (EDV) without changes in LV mass at end-diastolic phase (LVM) was observed in comparison to data from day 0 (EDV: 64.7 ± 9.8 *vs.* 56.8 ± 10.1 ml, $P=0.002$; LVM: 48.1 ± 4.6 *vs.* 47.1 ± 4.7 g, $P=0.3$; $n=10$). At day 7-9 a non-significant increase in end-systolic LV volume (ESV) was also noted (ESV: 44.1 ± 10.8 *vs.* 41.6 ± 8.1 ml, $P>0.05$). There was a close correlation between the relative extent of persistent MO in the infarct myocardium (% MO/MI) at day 0 and EDV at day 7-9 (Figure 3): $r=0.83$, $n=10$, $P=0.003$.

Discussion

The significance of microvascular obstruction has been demonstrated in many experimental and clinical studies and this entity has emerged as a therapeutic target in the clinical management of patients with reperfused AMI and after percutaneous coronary intervention, particularly saphenous vein graft interventions (13,14,24-26). Many factors affect the formation of microvascular obstruction in reperfused AMI. The high incidence of microvascular obstruction (>90%) in this experimental study was likely related to the prolonged duration of ischemia in the animals, which is a major determinant for the occurrence of microvascular obstruction



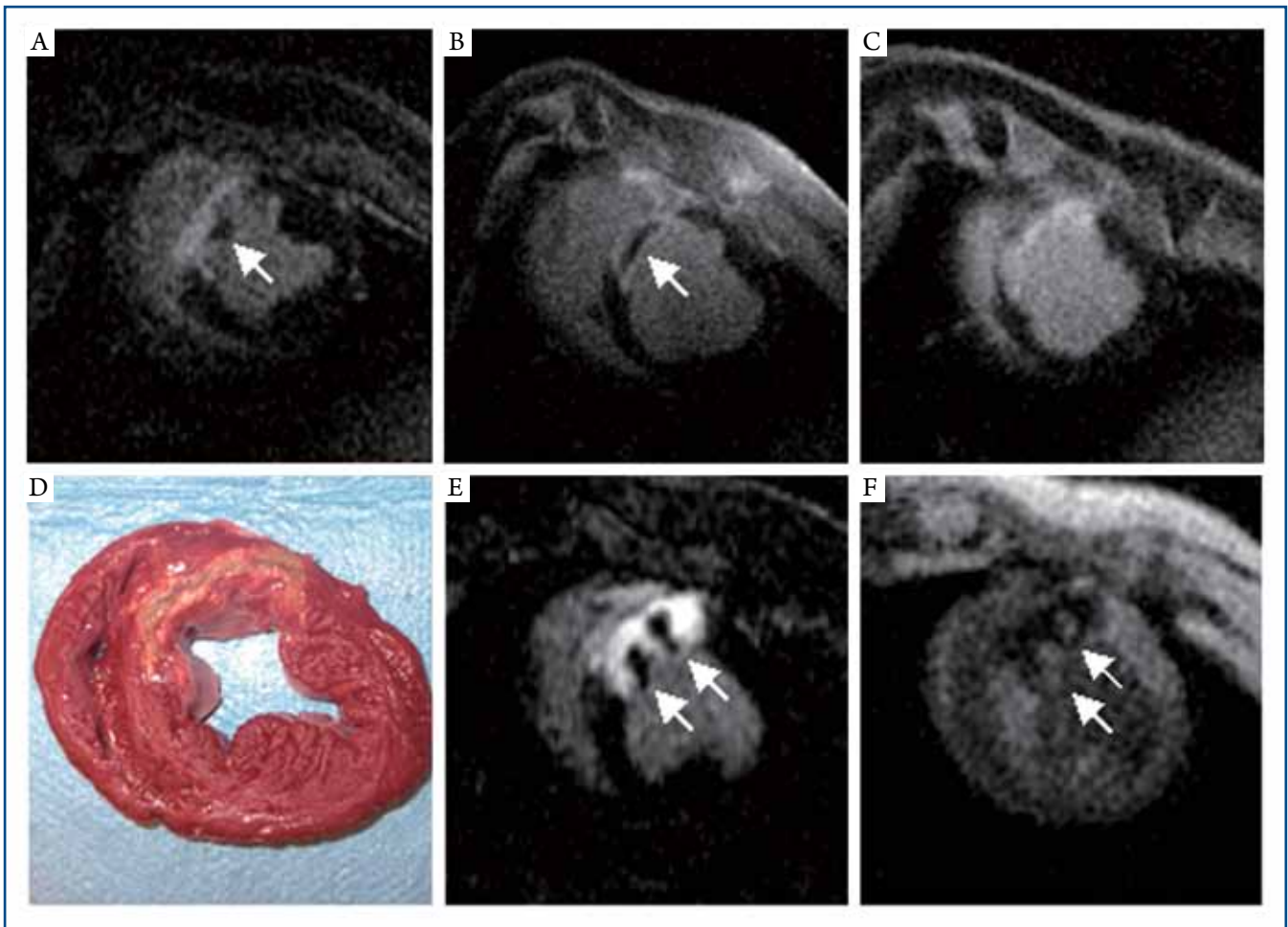


Figure 2. Varied MR appearances and progression of persistent MO (MO indicated by arrows; animal #1: A-D; animal #2: E-F). A: DE-MRI at day 0: MO predominantly in subendomyocardial region; B (DE-MRI at day 2): MO as a core within the MI region and with an increased volume; C: DE-MRI at day 7: MO is no longer seen; D: TTC staining confirming the presence of myocardial infarction; E-F: Multiple foci of MO on DE-MRI (E) and T1 Preparation difference image (F) at day 0. Note that MO appears as a hypo-enhanced region on DE-MRI and as a positive contrast on T1 difference image.

(3,27,28). Two fundamental mechanisms have been identified for microvascular obstruction: one occurring at the capillary level and characterized by myocardial necrosis and reperfusion damage; and the other occurring during the percutaneous coronary interventions due to distal embolization of plaque or thrombus (1,3,29). Microembolization is less likely the cause of obstruction in this study due to the use of anticoagulants and the fact that no thrombi (i.e. no filling defect) were observed on angiograms.

Many techniques have been used to delineate microvascular obstruction (2,4,17,29-31). TIMI flow grade is a simple and valuable way to diagnose microvascular obstruction or no-reflow phenomenon using angiography, especially when it arises from

the rupture of lipid-rich vulnerable plaques during percutaneous coronary intervention procedures and catheter-based protection devices might be the solution for this. However, this method often over-estimates the success of percutaneous coronary intervention because it only verifies the patency of the infarct-related artery, and not the re-establishment of tissue perfusion. In this experimental study, all ten animals with persistent microvascular obstruction identified using MRI had a TIMI flow grade 3 as demonstrated on angiography; this suggests that TIMI flow grade underestimates the incidence of microvascular obstruction and is not a good indicator of complete myocardial perfusion. This finding is consistent with previous works by other groups (32,33). TIMI myocardial blush score may be



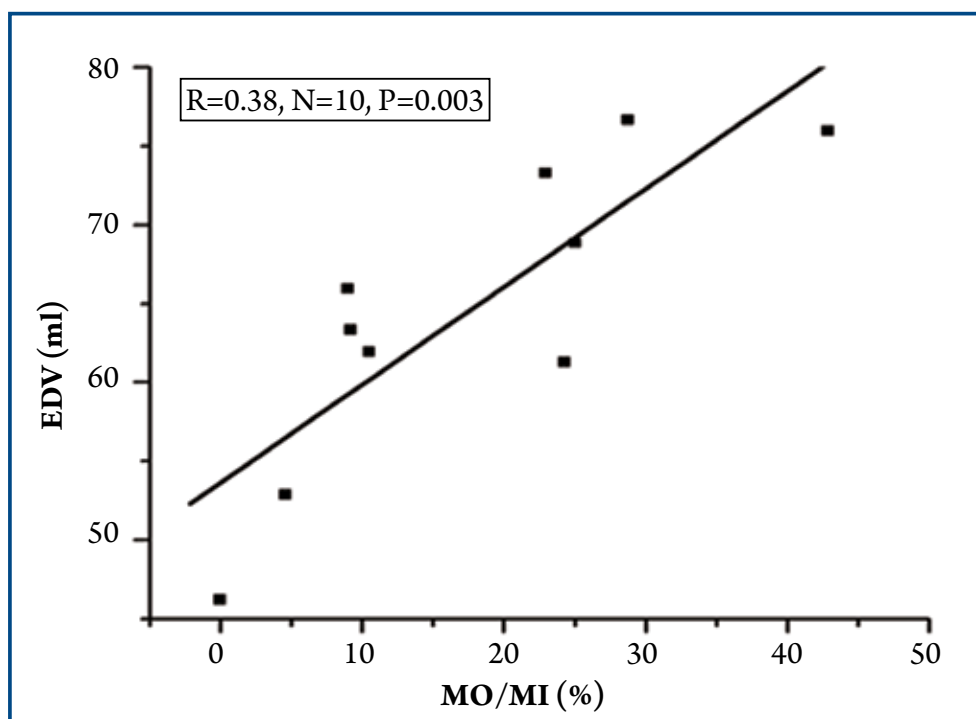


Figure 3. Correlation between the relative extent of persistent MO in the infarct myocardium (% MO/MI) at day 0 and end-diastolic volume at day 7-9.

a better angiographic method to evaluate the completeness of tissue perfusion (i.e. measuring the filling and clearance of contrast in myocardium) if the TIMI flow grade reaches 3, but this measurement requires more ionizing radiation and has limited sensitivity (34,35).

MRI is a validated non-invasive technique for the evaluation of myocardial viability and appears to be the most promising method for the accurate detection and quantitative measurement of microvascular obstruction in reperfused AMI (8-10). Multiple MRI techniques have been successfully applied in the diagnosis and follow-up of microvascular obstruction. FPMP and DE-MRI are sensitive techniques demonstrating microvascular obstruction as a hypo-enhanced region within reperfused AMI (10,15,17). In this study, a modified T1 preparation sequence post-contrast was used to delineate the microvascular obstruction as areas of positive contrast bounded by regions of dark infarcted tissue, which obviates partial volume effects associated with the high signal intensity from the adjacent infarct myocardium affecting the demonstration of microvascular obstruction. This positive contrast originated from a reduced gadopentetate dimeglumine distribution volume in microvascular obstruction relative to hyper-enhanced infarct regions, based on results from previous experimental studies (18).

In this experimental study, the progression and various MRI manifestations of microvascular obstruction were investigated during the short time course of infarct evolution from day 0 to day 7-9. Our results indicate that detection sensitivity for microvascular obstruction might be greatest around day 2 after reperfused AMI. In one animal, microvascular obstruction was not observed at day 0, but was visible at day 2, and the extent of microvascular obstruction was generally larger at day 2 than at day 0, although statistical significance was not reached. Rochitte *et al.* also noticed that the extent of microvascular obstruction increased significantly over the first 48 hours after myocardial infarction, indicating the presence of progressive microvascular dysfunction well beyond the coronary artery recanalization (23). In our study, persistent microvascular obstruction was noted in early DE-MRI but not visualized on late DE-MRI and T1 difference images post-contrast at day 7-9; which supports the belief that an early sub-acute time-point is superior for the demonstration of microvascular obstruction. Some model differences may exist — a rat model of ischemia/reperfusion has demonstrated a prolonged persistence of no-reflow phenomenon to at least four weeks (12).

Varied appearances were observed during the evolution of microvascular obstruction from day 0 to day 2. In one animal,



a predominantly subendocardial PMO progressed into a mid-myocardial core surrounded by infarct tissue. This progression is consistent with the wave-front pattern of evolution of myocardial infarction (36). As microvascular obstruction usually represents the myocardial region that experienced the most severe ischemic event and the subendomyocardial region is the area most sensitive to ischemia, it is expected that the subendomyocardial region may be the first site for the occurrence of microvascular obstruction following a long duration of ischemia. As the presence of microvascular obstruction indicates continued ischemia despite reperfusion, the extent of microvascular obstruction may expand into the mid-myocardium forming a core of no-reflow zone surrounded by infarct tissue, which is visualized as a core of hypo-enhancement with a rim of hyper-enhancement on DE-MRI images while on T1 difference images it is shown as a core of positive contrast with a dark rim of infarct tissue. A subendocardial obstruction zone was not observed in the majority of our animals; rather the mid-myocardial "core" pattern was observed, which is consistent with the severe ischemic injury. One animal presented with PMO at sub-acute time-points but not at day 0, which suggests either a subtle or small early subendomyocardial pattern of obstruction and significant evolution of the injury between day 0 and day 2.

The mechanism of occurrence of multiple distributions of microvascular obstruction in one animal is also not clear and may relate to the inherent heterogeneity of myocardial perfusion and metabolism (37). Perfusion heterogeneity may also complicate the establishment of a blood-tissue equilibrium distribution of gadolinium chelates during a constant infusion, indicated by an initial variability in contrast enhancement patterns after bolus contrast agent administration (38,39).

Negative LV remodeling due to microvascular obstruction was observed in this study. Compared to day 0, a significantly increased EDV and a mild but non-significantly increased ESV was observed at day 7-9. Linear regression analysis also demonstrated a close correlation between the relative extent of persistent microvascular obstruction in the infarct tissue and EDV at day 7-9 ($r=0.83$, $P=0.003$). In comparison, Gerber *et al.* evaluated LV remodeling in a canine model of microvascular obstruction using a 3D-tagging MRI technique (40). The MRI tagging findings demonstrated an increased regional myocardial stiffness in the microvascular obstruction segments from which adverse LV remodeling may originate, as proposed previously by Beyersdorf *et al.* (41). The consequent increased wall stress in the bordering peri-infarct zone may then provoke adverse remodeling of viable left ventricular muscle (42).

In this study, a more comprehensive characterization of PMO would have been achieved by incorporation of standard

histopathological techniques, such as Thioflavin-S infusion to define the extent of PMO, or radioactive microspheres to quantify regional blood flow (5,43). That said, first pass myocardial perfusion and DE-MRI are the gold standards for PMO detection in clinical populations (8-11,15), and hence it is useful to explore directly the role of these methods in delineating microvascular obstruction.

In conclusion, a varied MR appearance of persistent microvascular obstruction was observed during a short time course MRI study of reperfused acute myocardial infarction in a porcine model. The optimal time for detection of persistent microvascular obstruction is unknown but may be around 48 hours after infarction. Adverse left ventricular remodeling was closely related to the relative extent of persistent microvascular obstruction of the infarct myocardium. Thus early intervention to improve the clinical prognosis associated with microvascular obstruction may be guided by MR imaging studies.

References

1. Kloner RA. Foreword-No-reflow: Basic science to a clinical phenomenon. *Basic Res Cardiol* 2006;10:357-8.
2. Luo AK, Wu KC. Imaging microvascular obstruction and its clinical significance following acute myocardial infarction. *Heart Fail Rev* 2006;11:305-12.
3. Reffelmann T, Kloner RA. The no-reflow phenomenon: A basic mechanism of myocardial ischemia and reperfusion. *Basic Res Cardiol* 2006;101:359-72.
4. Young JJ, Cox DA, Stuckey T, et al. Prospective, multicenter study of thrombectomy in patients with acute myocardial infarction: the X-Tract AMI registry. *J Interv Cardiol* 2007;20:44-50.
5. Kloner RA, Ganote CE, Jennings RB. The "no-reflow" phenomenon after temporary coronary occlusion in the dog. *J Clin Invest* 1974;54:1496-508.
6. Camilleri JP, Joseph D, Fabiani JN, et al. Microcirculatory changes following early reperfusion in experimental myocardial infarction. *Virchows Arch A Pathol Anat Histol* 1976;369:315-33.
7. Eeckhout E, Kern MJ. The coronary no-reflow phenomenon: a review of mechanisms and therapies. *Eur Heart J* 2001;22:729-39.
8. Bogaert J, Kalantzi M, Rademakers FE, et al. Determinants and impact of microvascular obstruction in successfully reperfused ST-segment elevation myocardial infarction. Assessment by magnetic resonance imaging. *Eur Radiol* 2007;17:2572-80.
9. Wu KC, Zerhouni EA, Judd RM, et al. Prognostic significance of microvascular obstruction by magnetic resonance imaging in patients with acute myocardial infarction. *Circulation* 1998;97:765-72.
10. Hombach V, Grebe O, Merkle N, et al. Sequelae of acute myocardial infarction regarding cardiac structure and function and their prognostic significance as assessed by magnetic resonance imaging. *Eur Heart J*



- 2005;26:549-57.
11. Lombardo A, Niccoli G, Natale L, et al. Impact of microvascular obstruction and infarct size on left ventricular remodeling in reperfused myocardial infarction: a contrast-enhanced cardiac magnetic resonance imaging study. *Int J Cardiovasc Imaging* 2011. [Epub ahead of print]
 12. Reffelmann T, Hale SL, Dow JS, et al. No-reflow phenomenon persists long-term after ischemia/reperfusion in the rat and predicts infarct expansion. *Circulation* 2003;108:2911-7.
 13. Schwartz RS. Microvascular obstruction in acute coronary syndromes: onward to a new therapeutic target. *Catheter Cardiovasc Interv* 2005;66:170-2.
 14. Topol EJ, Yadav JS. Recognition of the importance of embolization in atherosclerotic vascular disease. *Circulation* 2000;101:570-80.
 15. Lund GK, Stork A, Saeed M, et al. Acute myocardial infarction: evaluation with first-pass enhancement and delayed enhancement MR imaging compared with 201TI SPECT imaging. *Radiology* 2004;232:49-57.
 16. Wu KC, Kim RJ, Bluemke DA, et al. Quantification and time course of microvascular obstruction by contrast-enhanced echocardiography and magnetic resonance imaging following acute myocardial infarction and reperfusion. *J Am Coll Cardiol* 1998;32:1756-64.
 17. Albert TS, Kim RJ, Judd RM. Assessment of no-reflow regions using cardiac MRI. *Basic Res Cardiol* 2006;101:383-90.
 18. Yang Y, Foltz W, Graham J, et al. Microvascular obstruction in an experimental reperfused acute myocardial infarction at the very early stage: evaluation using a modified T1 Prep Look-locker sequence. *J Cardiovasc Magn Reson* 2006;8:118-20.
 19. Thornhill RE, Prato FS, Wisenberg G, et al. Determining the extent to which delayed-enhancement images reflect the partition-coefficient of Gd-DTPA in canine studies of reperfused and unperfused myocardial infarction. *Magn Reson Med* 2004;52:1069-79.
 20. Foltz WD, Yang Y, Graham JJ, et al. MRI relaxation fluctuations in acute reperfused hemorrhagic infarction. *Magn Reson Med* 2006;56:1311-9.
 21. Yang Y, Foltz WD, Graham JJ, et al. MRI evaluation of microvascular obstruction in experimental reperfused acute myocardial infarction using a T1 and T2 preparation pulse sequence. *J Magn Reson Imaging* 2007;26:1486-92.
 22. Holman ER, Vliegen HW, van der Geest RJ, et al. Quantitative analysis of regional left ventricular function after myocardial infarction in the pig assessed with cine magnetic resonance imaging. *Magn Reson Med* 1995;34:161-9.
 23. Rochitte CE, Lima JA, Bluemke DA, et al. Magnitude and time course of microvascular obstruction and tissue injury after acute myocardial infarction. *Circulation* 1998;98:1006-14.
 24. Ito H, Maruyama A, Iwakura K, et al. Clinical implications of the 'no reflow' phenomenon. A predictor of complications and left ventricular remodeling in reperfused anterior wall myocardial infarction. *Circulation* 1996;93:223-8.
 25. Resnic FS, Wainstein M, Lee MK, et al. No-reflow is an independent predictor of death and myocardial infarction after percutaneous coronary intervention. *Am Heart J* 2003;145:42-6.
 26. Keeley EC, Velez CA, O'Neill WW, et al. Long-term clinical outcome and predictors of major adverse cardiac events after percutaneous interventions on saphenous vein grafts. *J Am Coll Cardiol* 2001;38:659-65.
 27. Reffelmann T, Hale SL, Li G, et al. Relationship between no reflow and infarct size as influenced by the duration of ischemia and reperfusion. *Am J Physiol Heart Circ Physiol* 2002;282:H766-72.
 28. Tarantini G, Cacciavillani L, Corbetti F, et al. Duration of ischemia is a major determinant of transmural and severe microvascular obstruction after primary angioplasty: a study performed with contrast-enhanced magnetic resonance. *J Am Coll Cardiol* 2005;46:1229-35.
 29. Ito H. No-reflow phenomenon and prognosis in patients with acute myocardial infarction. *Nat Clin Pract Cardiovasc Med* 2006;3:499-506.
 30. Kaul S. Evaluating the 'no reflow' phenomenon with myocardial contrast echocardiography. *Basic Res Cardiol* 2006;101:391-9.
 31. Jeremy RW, Links JM, Becker LC. Progressive failure of coronary flow during reperfusion of myocardial infarction: documentation of the no reflow phenomenon with positron emission tomography. *J Am Coll Cardiol* 1990;16:695-704.
 32. Stone GW, Peterson MA, Lansky AJ, et al. Impact of normalized myocardial perfusion after successful angioplasty in acute myocardial infarction. *J Am Coll Cardiol* 2002;39:591-7.
 33. Choi JW, Gibson CM, Murphy SA, et al. Myonecrosis following stent placement: association between impaired TIMI myocardial perfusion grade and MRI visualization of microinfarction. *Catheter Cardiovasc Interv* 2004;61:472-6.
 34. Perez de Prado A, Fernández-Vázquez F, Cuellas-Ramón JC, et al. Coronary clearance frame count: a new index of microvascular perfusion. *J Thromb Thrombolysis* 2005;19:97-100.
 35. Greaves K, Dixon SR, Fejka M, et al. Myocardial contrast echocardiography is superior to other known modalities for assessing myocardial reperfusion after acute myocardial infarction. *Heart* 2003;89:139-44.
 36. Reimer KA, Jennings RB. The "wavefront phenomenon" of myocardial ischemic cell death. II. Transmural progression of necrosis within the framework of ischemic bed size (myocardium at risk) and collateral flow. *Lab Invest* 1979;40:633-44.
 37. Bassingthwaite JB, Beard DA, Li Z. The mechanical and metabolic basis of myocardial blood flow heterogeneity. *Basic Res Cardiol* 2001;96:582-94.
 38. Flacke SJ, Fischer SE, Lorenz CH. Measurement of the gadopentetate dimeglumine partition coefficient in human myocardium in vivo: normal distribution and elevation in acute and chronic infarction. *Radiology* 2001;218:703-10.
 39. Thornhill RE, Prato FS, Wisenberg G, et al. Determining the extent to which delayed-enhancement images reflect the partition-coefficient of Gd-DTPA in canine studies of reperfused and unperfused myocardial infarction. *Magn Reson Med* 2004;52:1069-79.
 40. Gerber BL, Rochitte CE, Melin JA, et al. Microvascular obstruction and left



- ventricular remodeling early after acute myocardial infarction. *Circulation* 2000;101:2734-41.
41. Beyersdorf F, Okamoto F, Buckberg GD, et al. Studies on prolonged acute regional ischemia. II. Implications of progression from dyskinesia to akinesia in the ischemic segment. *J Thorac Cardiovasc Surg* 1989;98:224-33.
 42. Kramer CM, Lima JA, Reichek N, et al. Regional differences in function within noninfarcted myocardium during left ventricular remodeling. *Circulation* 1993;88:1279-88.
 43. Judd RM, Lugo-Olivieri CH, Arai M, et al. Physiological basis of myocardial contrast enhancement in fast magnetic resonance images of 2-day-old reperfused canine infarcts. *Circulation* 1995;92:1902-10.

Cite this article as: Yang Y, Graham JJ, Connelly K, Foltz WD, Dick AJ, Wright G. MRI MRI manifestations of persistent microvascular obstruction and acute left ventricular remodeling in an experimental reperfused myocardial infarction. *Quant Imaging Med Surg* 2012;2:12-20. DOI: 10.3978/j.issn.2223-4292.2011.12.02

